Characterizing the Small-Scale Fading for Low Altitude UAV Channels

Xuesong Cai[†‡], Jian Song[†], José Rodríguez-Piñeiro[*], Preben E. Mogensen[†♮], and Fredrik Tufvesson[‡]

[†]Department of Electronic Systems, Aalborg University, Aalborg, Denmark, {xuc, jians, pm}@es.aau.dk
[*]College of Electronics and Information Engineering, Tongji University, Shanghai, China, j.rpineiro@tongji.edu.cn
[♮]Nokia, Aalborg, Denmark.
[‡]Department of Electrical and Information Technology, Lund University, Lund, Sweden,
{xuesong.cai, fredrik.tufvesson}@eit.lth.se

***Abstract*—In this contribution, a recently conducted measurement campaign in a suburban scenario for the Unmanned Aerial Vehicle (UAV) Air-to-Ground (A2G) radio channel is introduced. The downlink signals in an in-service Long Term Evolution (LTE) network were collected and utilized to extract the Channel Impulse Responses (CIRs). A high-resolution parameter estimation algorithm derived based on the Space-Alternating Generalized Expectation-maximization (SAGE) principle is applied to estimate the delays, Doppler frequencies and complex amplitudes of MultiPath Components (MPCs) from the CIRs. Based on the MPC estimation results, fast fading characteristics of the A2G channels are investigated. It is found that the Rician distribution models the fast fading the best compared to Nakagami, Lognormal and Rayleigh distributions. Rician K-factors are also calculated for the A2G channels.**

Keywords- UAV; air-to-ground; LTE; multipath components; fast fading.

I. INTRODUCTION

Unmanned Aerial Vehicles (UAVs) have recently attracted a surge of research interest. They can be exploited as aerial Base Stations (BS) [1] and/or aerial user equipments [2] to enable various applications such as sensing, delivery, etc. [3]. There has been a certain amount of works conducted to understand the Air-to-Ground (A2G) channels, e.g., in [2], [4]–[10] and references therein. Channel characteristics including path loss, delay dispersions, Doppler spread, etc. were investigated. It is worth noting that the first comprehensive measurement-based angular characterization of the A2G channels was carried out in [4]. Although some previous works characterized the small-scale fading, i.e., fast fading, using the Rician K factor, it is not known whether the Rician distribution is really suitable for the A2G channels. In this contribution, we conduct measurement-based analysis, to see which distribution is the most suitable for modeling the fast fading. The rest of this paper is structured as follows. The measurement equipment, scenario and raw data processing are described in Section II. Section III elaborates the investigation on the fast fading behavior. Finally, conclusive remarks are drawn in Section IV.

II. MEASUREMENT EQUIPMENT, SCENARIO, AND RAW DATA PROCESSING

The measurement equipment, scenario, CIR extraction and MPC parameter estimation are briefly introduced in this section. Detailed information can also be found in [6].

A. Transmitter and receiver

In the measurement campaign, a commercial Frequency Division Duplexing Long Term Evolution (FDD-LTE) base station was exploited as the transmitter with its real-time downlink signals collected by the receiver. The receiver system mainly consisted of the following components: a UAV, a Universal-Software-defined Radio-Peripheral (USRP) device of type B210 [11], an Oven-Controlled Crystal Oscillator (OCXO), a cube Lenovo computer, an omnidirectional antenna and three lithium batteries. The OCXO provided a stable local oscillator for the USRP. The cube computer controlled the USRP via the GNU radio software and stored the received data. These components were loaded on the UAV fixed tightly as illustrated in in Figure 1(a).

B. Measurement scenario

The measurement was performed in the suburban scenario as illustrated in Figure 1(c). There were several tall buildings and many metal containers with lower heights. The LTE base station was located in front of and almost in the Line-of-Sight (LoS) of the UAV. The carrier frequency of the LTE downlink signals was 1.8 GHz, and the bandwidth was 13.5 MHz. The UAV flied vertically from the ground to the height of 50 m in about 35 seconds as indicated in Figure 1(b). The signals were acquired by using the USRP with a sample rate of 30.72 MHz. Due to the hardware data steaming limitations, the data were stored in fragments each lasting 15 seconds.

C. Raw data processing

The CIRs were extracted from the Cell Specific Signals (CRSs) as elaborated in [2], [12]. Briefly, synchronization and physical cell detection were first done. With the transmitted CRSs known according to [13], the channel transfer functions can be calculated, and so the CIRs. The signal model of a CIR in the SAGE algorithm [14] is formulated as

$$h(t,\tau) = \sum_{\ell=1}^{L} \alpha_\ell(t)\delta(\tau - \tau_\ell(t)) \exp\left\{ j2\pi \int_0^t \nu_\ell(t)dt \right\}, \quad (1)$$

where L, $\alpha_\ell(t)$, $\tau_\ell(t)$, and $\nu_\ell(t)$ denote the number of paths, complex amplitudes, delays and Doppler frequencies, respectively, and $\delta(\cdot)$ is the Dirac delta function. Four consecutive CIRs were considered as one snapshot. The SAGE algorithm was applied with $L = 18$ that was found proper to fully extract the dominant MPCs in each snapshot.

 ISBN: 978-1-61208-878-5

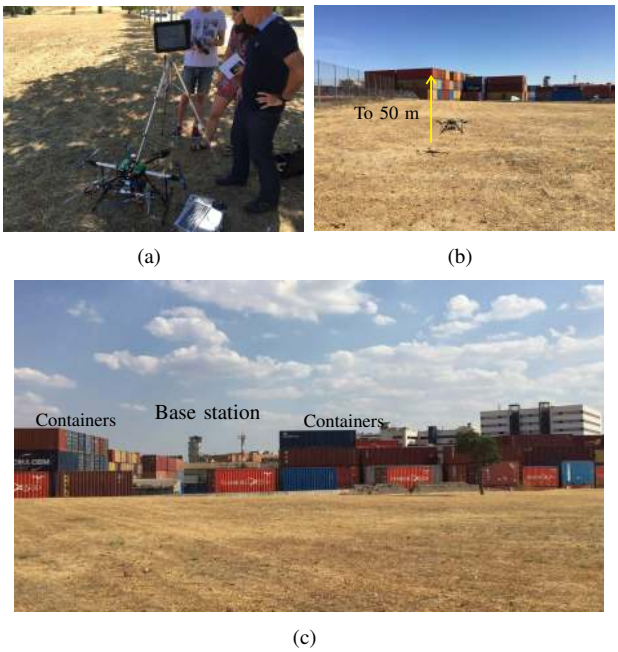

(a) (b)

(c)

Figure 1. The measurement equipments and scenario. a) All the components used in the experiments. b) The UAV was flying from the ground to the air. c) The surroundings of the scenario.

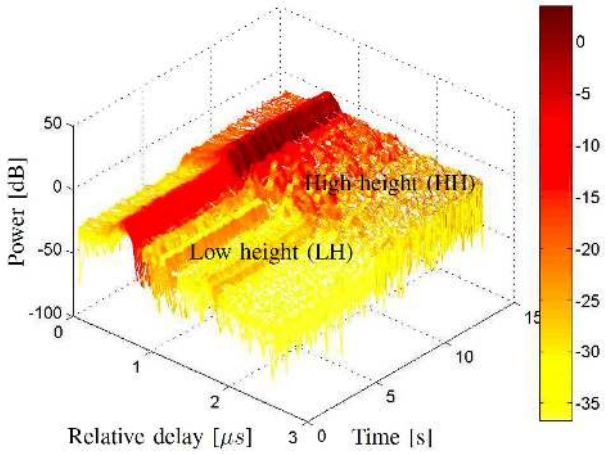

Figure 2. An example concatenated PDPs lasting 15 seconds [6].

III. Small-scale fading

As illustrated in Figure 2, we first show concatenated power-delay-profiles (PDPs) lasting 15 s that correspond to the UAV flying from the ground to the air. It can be observed that the channels before and after 7.5 seconds are different. We use Low Height (LH) and High Height (HH) to distinguish them. Our conjecture [6] for the difference is that when the height was low, the UAV could only receive the LoS signals and the signals reflected from buildings with high heights or side walls of containers. However, when the UAV flied high above the containers and buildings, signals reflected from the roofs started impinging into the UAV, and the signal power also increased. The SAGE estimation results are also illustrated in Figure 3 for the example channel shown in Figure 2.

Based on the SAGE estimation results, the channel fading

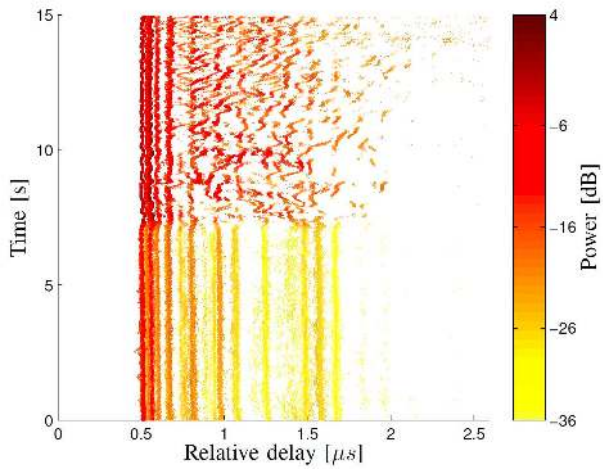

Figure 3. The SAGE estimation results for the channels as illustrated in Figure 2 [6].

amplitude is calculated as

$$G = \sum_{\ell=1}^{L} \alpha_\ell. \quad (2)$$

To fully understand the small-scale fading behaviors, Akaike's Information Criteria (AIC) is applied to select the best fitting model for the fading amplitudes in both cases, among all the J ($J = 4$) candidate distributions: Rician, Nakagami, Log-normal and Rayleigh. AIC is a measure of the relative fitting goodness of a statistical model, and is widely used in the wireless communications [15], [16]. Akaike weights derived from AICs which satisfy $\sum_{i=1}^{J} \omega_j = 1$ are applied to select the best distribution with the largest Akaike weight. We choose 80 SAGE snapshots to obtain reliable Akaike weights. Note that $N/U \geq 40$ should be satisfied to obtain reliable Akaike weights, where N is the sample number, U is the number of free model parameter(s). Readers are referred to [16] for elaborated discussions about AIC. The distance that the UAV moves in 80 SAGE snapshots is about 4 times the half wavelength, which is in the small-scale level. Figs. 4(a) and 4(b) illustrate the AIC weights for the four candidate distributions in the LH and HH cases respectively. It can be observed that in both cases, the Rician distribution best fits the small-scale fading, the goodness of Nakagami and Log-normal distributions is similar, and the Rayleigh distribution is not suitable for modelling the fading behaviors. Furthermore, the best fitting rate of Rician distribution in the HH case (70.9%) is lower than that of the LH case (74.3%). This is consistent with the fact that the HH channel measured in this specific scenario herein includes more non-negligible MPCs.

Since the Rician distribution has the best goodness of fit in both cases and is commonly used to model the propagation channel with a dominant path, the Rician K-factor is investigated by using the moment-based method, specified in [17],

 ISBN: 978-1-61208-878-5

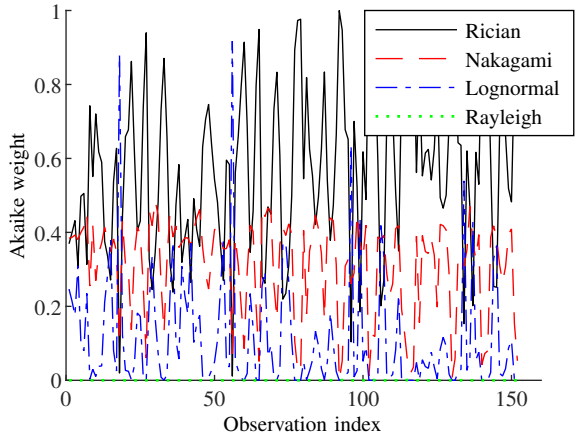

(a)

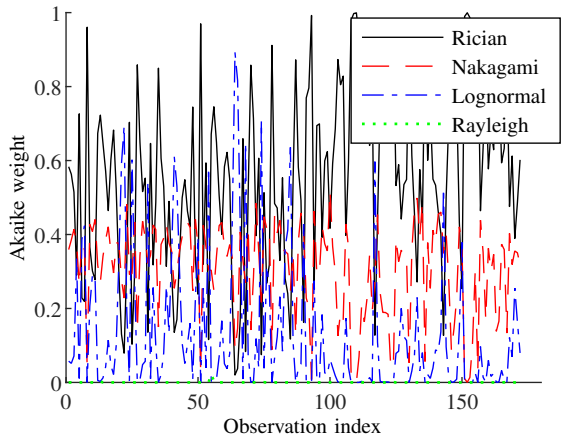

(b)

Figure 4. Akaike weights for the four candidates in the LH case and the HH case. a) LH case. Rician 74.3% best, Nakagami 19.2% best, Lognormal 6.5% best, and Rayleigh 0% best. b) HH case. Rician 70.9% best, Nakagami 15.7% best, Lognormal 13.4% best, and Rayleigh 0% best.

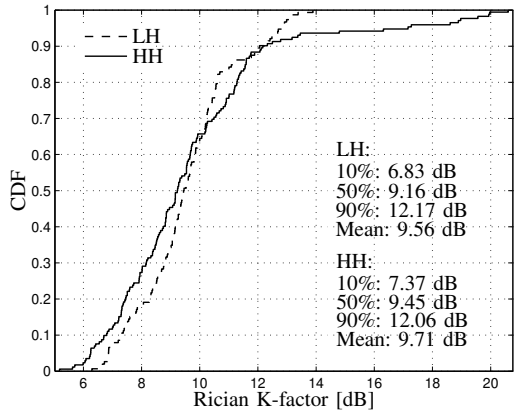

Figure 5. CDFs for Rician K-factors in the LH case and the HH case.

as

$$K = \frac{\sqrt{1 - \frac{\mathrm{Var}[G^2]}{(\mathrm{E}[G^2])^2}}}{1 - \sqrt{1 - \frac{\mathrm{Var}[G^2]}{(\mathrm{E}[G^2])^2}}}, \tag{3}$$

where $\mathrm{Var}(\cdot)$ and $\mathrm{E}(\cdot)$ represent the variance and the expectation of the argument, respectively. Figure 5 illustrates the CDFs for the K-factors in the LH and HH cases respectively. It can be observed that the HH K-factor is smaller than the LH K-factor under the 65% level. This is consistent with the fact that the more MPCs with non-negligible powers in the HH case can sometimes result in more severe fading compared to the LH case. However, the maximum HH K-factor is larger than that of the LH case. This is also understandable since the blockage to the LoS path is lower.

IV. Conclusions

The low altitude UAV radio channel in a suburban scenario was investigated. Based on the downlink data received from a commercial LTE base station, high resolution estimation results of multipath components were obtained using the SAGE algorithm. Based on the SAGE estimation results, fast fading behaviors were analyzed. Among Rician, Nagakami, Lognormal and Rayleigh distributions, it has been found that the Rician distribution can best model the fast fading of the UAV channel with a best-fitting rate of more than 70%. Moreover, large Ricean K-factors, with average values of 10 dB and maximum ones of 20 dB, were found. In addition, it is interesting to find that in this special suburban scenario, the UAV channel became less Los-dominant (probably due to the reflections at the roofs of buildings and metallic containers), which is different from the common belief that the A2G channel at a higher hight should be more LoS-dominant.

Acknowledgement

The authors wish to express their thanks to Prof. Cesar Briso at the Technical University of Madrid for his help in conducting the measurement. The work of José Rodríguez-Piñeiro is supported in part by the National Natural Science Foundation of China (NSFC) under Grant 61971313, and in part by the Sino-German Center of Intelligent Systems, Tongji University, Shanghai, China.

References

[1] N. Babu, C. B. Papadias, and P. Popovski, "Energy-efficient 3-D deployment of aerial access points in a UAV communication system," *IEEE Communications Letters*, vol. 24, no. 12, pp. 2883–2887, 2020.

[2] X. Cai *et al.*, "An empirical air-to-ground channel model based on passive measurements in LTE," *IEEE Transactions on Vehicular Technology*, vol. 68, no. 2, pp. 1140–1154, 2019.

[3] S. Hayat, E. Yanmaz, and R. Muzaffar, "Survey on unmanned aerial vehicle networks for civil applications: A communications viewpoint," *IEEE Communications Surveys Tutorials*, vol. 18, no. 4, pp. 2624–2661, 2016.

[4] X. Cai *et al.*, "Empirical low-altitude air-to-ground spatial channel characterization for cellular networks connectivity," *IEEE Journal on Selected Areas in Communications*, pp. 1–1, 2021.

 ISBN: 978-1-61208-878-5

[5] ——, "Interference modeling for low-height air-to-ground channels in live LTE networks," *IEEE Antennas and Wireless Propagation Letters*, vol. 18, no. 10, pp. 2011–2015, 2019.

[6] ——, "Low altitude UAV propagation channel modelling," in *11th European Conference on Antennas and Propagation (EUCAP)*, 2017, pp. 1443–1447.

[7] C. Yan, L. Fu, J. Zhang, and J. Wang, "A comprehensive survey on UAV communication channel modeling," *IEEE Access*, vol. 7, pp. 107 769–107 792, 2019.

[8] J. Rodríguez-Piñeiro, Z. Huang, X. Cai, T. Domínguez-Bolaño, and X. Yin, "Geometry-based mpc tracking and modeling algorithm for time-varying UAV channels," *IEEE Transactions on Wireless Communications*, vol. 20, no. 4, pp. 2700–2715, 2021.

[9] J. Rodríguez-Piñeiro, T. Domínguez-Bolaño, X. Cai, Z. Huang, and X. Yin, "Air-to-ground channel characterization for low-height UAVs in realistic network deployments," *IEEE Transactions on Antennas and Propagation*, vol. 69, no. 2, pp. 992–1006, 2021.

[10] Z. Huang, J. Rodríguez-Piñeiro, T. Domínguez-Bolaño, X. Cai, and X. Yin, "Empirical dynamic modeling for low-altitude UAV propagation channels," *IEEE Transactions on Wireless Communications*, pp. 1–1, 2021.

[11] "USRP B210 Datasheet," Tech. Rep. [Online]. Available: https://www.ettus.com/product/details/UB210-KIT, 2021.

[12] X. Ye, X. Cai, Y. Shen, X. Yin, and X. Cheng, "A geometry-based path loss model for high-speed-train environments in LTE-A networks," in *2016 International Conference on Computing, Networking and Communications (ICNC)*, Feb 2016, pp. 1–6.

[13] *Technical Specification Group Radio Access Network; Evolved Universal Terrestrial Radio Access (E-UTRA); Physical channels and modulation*, 3rd Generation Partnership Project 3GPP TS 36.211 V13.2.0 (2016-07) Std.

[14] B. Fleury, M. Tschudin, R. Heddergott, D. Dahlhaus, and K. Ingeman Pedersen, "Channel parameter estimation in mobile radio environments using the SAGE algorithm," *IEEE Journal on Selected Areas in Communications*, vol. 17, no. 3, pp. 434–450, 1999.

[15] R. He *et al.*, "Short-term fading behavior in high-speed railway cutting scenario: Measurements, analysis, and statistical models," *IEEE Transactions on Antennas and Propagation*, vol. 61, no. 4, pp. 2209–2222, April 2013.

[16] U. G. Schuster and H. Bolcskei, "Ultrawideband channel modeling on the basis of information-theoretic criteria," *IEEE Transactions on Wireless Communications*, vol. 6, no. 7, pp. 2464–2475, July 2007.

[17] L. J. Greenstein, D. G. Michelson, and V. Erceg, "Moment-method estimation of the Ricean K-factor," *IEEE Communications Letters*, vol. 3, no. 6, pp. 175–176, June 1999.

 ISBN: 978-1-61208-878-5